

Hertzian Contact Response of Tailored Silicon Nitride Multilayers

Haiyan Liu, Brian R. Lawn, and Stephen M. Hsu

Materials Science and Engineering Laboratory, National Institute of Standards and Technology,
Gaithersburg, Maryland 20899

The nature and degree of damage accumulation beneath Hertzian contacts in silicon nitride-based laminates are studied. Specimens with alternating homogeneous and heterogeneous layers are fabricated by a tape-casting route, with strong interlayer bonding. Homogeneous material consisting of relatively pure fine-grain silicon nitride is used as the overlayers. Heterogeneous material containing 10 to 30 wt% boron nitride platelets in a silicon nitride matrix, with weak platelet/matrix interphase boundaries, forms the underlayers. Contact tests with spherical indenters are used to monitor the stress-strain response of the laminates and to investigate the damage modes within the individual layers. The heterogeneous layer exhibits a distinctive "softening" in the stress-strain curve, indicating a quasi-plasticity in the silicon nitride associated with local microfailures at the platelet/matrix interfaces. In contrast to the well-defined cone cracks that develop within the tensile zone outside the contact area in bulk homogeneous silicon nitride, the damage in the laminates is widely distributed within the shear-compression zone below the contact. Fractures form incompletely in the homogeneous layers, as downward-propagating partial cone cracks and upward-propagating stable cracks. Comparatively extensive, diffuse microscopic damage occurs in the heterogeneous layers, culminating in a macroscopic failure that traverses these layers at higher loads. A strong synergism between the interlayer damage modes is apparent. Implications concerning the design of composite laminates for improved damage tolerance, with retention of strength and wear resistance, are considered.

I. Introduction

SILICON NITRIDE is considered a potentially useful structural ceramic for its combination of toughness, strength, hardness, and chemical and thermal durability. However, in its conventional homogeneous fine-grain form, silicon nitride is not damage-tolerant. Generally, to increase damage tolerance in ceramics it is necessary to introduce heterogeneity into the microstructure.¹ One approach that has met with some success in silicon nitride is to include long, elongate grains, preferably by some *in situ* processing route.²⁻⁴ In that case the enhanced tolerance is attributable to crack bridging.⁴⁻⁷ Another way to improve damage tolerance is to introduce second-phase particulates into the silicon nitride matrix, notably platelets with weak cleavage planes or interphase boundaries, so as to distribute the damage.⁸ Hexagonal phase boron nitride platelets, with their weak basal cleavage, are especially effective in this regard.^{9,10} At the same time, increasing heterogeneity in ceramics runs the risk of degrading properties on the microscale.⁸ This tendency is illustrated most dramatically in Hertzian contact tests

in heterogeneous ceramics,¹¹⁻¹⁵ including silicon nitride;¹⁶⁻¹⁹ whereas in homogeneous brittle materials the contact produces a well-defined tensile cone crack, in heterogeneous solids it produces a diffuse "quasi-plastic" damage zone containing discrete shear faults.⁸ Consequently, heterogeneous microstructures are particularly susceptible to surface removal in repeated contacts, to the point of being "machinable."^{9,15,20,21} Hence, designing with silicon nitride may demand compromise, depending on whether one seeks toughness and flaw tolerance on one hand, or wear and fatigue resistance on the other.

One potential methodology for avoiding such compromise is to laminate the ceramic structure with an outermost homogeneous layer to provide wear resistance and an underlying heterogeneous layer to provide toughness. Traditionally, ceramic laminates have been designed to promote deflection at weak interlayer interfaces.²²⁻²⁹ However, deflection cracks degrade transverse strength and other properties. A newer philosophy, foreshadowed by the work of Marshall and others on alumina/zirconia³⁰⁻³² and alumina/monazite,³³ advocates incorporating strong interfaces between the adjoining layers, so that cracks do not delaminate but arrest or disperse as energy is absorbed within the heterogeneous layers. This conception of strongly bonded homogeneous/heterogeneous interlayers has been demonstrated most recently in an alumina-based trilayer structure,³⁴ where "yield" in a soft inner layer "shields" contact-induced cone cracks in a hard outer layer. The response is somewhat analogous to that of ceramic/metal layer composites,³⁵ but without the extreme elastic-plastic mismatch or high-temperature chemical incompatibility.

In this paper we present results of Hertzian contact tests on a multilayer laminate of homogeneous and heterogeneous silicon nitride produced in our laboratories. The layers are processed as tapes, which are co-hot-pressed to produce strong interlayer bonding. The homogeneous component is a relatively fine-grain material; the heterogeneous component is a silicon nitride matrix with coarse, chemically compatible boron nitride platelets, similar to composite structures described by others^{9,10} but with relatively low porosity and a textured platelet microstructure. Layer thicknesses are designed to be thin relative to the scale of contact, so that several layers may be sampled in any typical deformation. "Bonded-interface" sections through the Hertzian contact zone¹² are used to identify and characterize a complex distribution of accumulated microfracture in the homogeneous layers and deformation in the heterogeneous layers. Indentation stress-strain curves graphically illustrate the capacity of the laminate system to absorb energy from the loading system, particularly within the heterogeneous layer, and thereby to distribute damage.

II. Experimental Procedure

(1) Laminate Preparation

Silicon nitride (Si_3N_4) laminates with boron nitride (BN) additives were prepared by a sequence of tape casting, laminating, binder burnout, and hot pressing. The procedure was similar to that described in an earlier paper, except that there the BN was confined to a thin interlayer between thicker Si_3N_4 slabs, to provide a weak interface for delamination.³⁶ In the

R. O. Scattergood—contributing editor

Manuscript No. 192490. Received July 5, 1995; approved November 15, 1995.
Supported in part by the U.S. Air Force Office of Scientific Research.
Identification of commercial sources of materials or equipment in this paper does not imply recommendation or endorsement by NIST.

present experiments, BN was mixed with the Si_3N_4 starting powder in prescribed weight fractions, to produce heterogeneous interlayers for strong bonding with the homogeneous Si_3N_4 layers.

For the homogeneous layers, designated here as S, starting powders of pure Si_3N_4 (E10 powder, UBE Industries, Tokyo, Japan) plus 2.5 wt% MgO and 1 wt% Al_2O_3 (Aldrich Chemical, Milwaukee, WI) sintering additives and a commercial binder (B73305, Metoramic Sciences, Carlsbad, CA) were ball-milled for 24 h. For the heterogeneous layers, designated B, powders of Si_3N_4 (SNE powder, Denka, Japan) were mixed with either 10 wt% or 30 wt% hexagonal BN (Aldrich) plus 5 wt% Y_2O_3 and 5 wt% Al_2O_3 (Aldrich) sintering additives and binder, and similarly ball-milled to produce B10 or B30 composites. The slurries were cast into tapes, dried, and punched into slabs 50 mm \times 50 mm. The resulting slabs were stacked in alternating homogeneous/heterogeneous layers, with the homogeneous layers on the outside, and heated to 80°C under 20 MPa for 10 min to form green bodies. After a burnout cycle to 400°C to remove the binder, the laminates were given a final hot press at 1770°C under 30 MPa for 1.5 h, producing blocks of final thickness \approx 3 mm.

The generic structure of the resultant SB10 and SB30 laminates is depicted schematically in Fig. 1, with layer thicknesses as summarized in Table I. Additionally, some reference specimens of similar thickness were prepared of the bulk Si_3N_4 S material and each of the composite B10 and B30 materials for baseline tests.

Cross sections were cut and polished to 1 μm finish for microstructural evaluation. X-ray diffraction was used to identify the phases of the layers in these section specimens. Microscopy was carried out by scanning electron microscopy (SEM). The microstructural texture was revealed most clearly by gold-coating the section surfaces after a plasma etch treatment. Porosities of each of the constituent layer materials were evaluated using the Archimedes method.

Exploratory Vickers indentations were made in the B30 composite surfaces, to observe the influence of the BN second phase in radial crack propagation.

(2) Hertzian Indentation Testing

Hertzian indentation tests were made using tungsten carbide spheres on polished SB laminate top surfaces (Fig. 1) as well as on bulk S and B specimens. Initial tests were made to determine indentation stress–strain curves.^{12,13} Test surfaces were coated with gold before indentation, to facilitate measurement of residual contact radius a . This enabled determination of an indentation stress, $p_0 = P/\pi a^2$, and indentation strain, a/r , for each contact. Data were taken using a range of sphere radius $r = 1.59$ to 12.7 mm, at loads up to $P = 3000$ N, in order to construct the stress–strain curves.

To reveal the subsurface damage, a special bonded-interface configuration was used.^{11,13} Polished surfaces of two half-specimens were glued face-to-face with a thin layer of adhesive under light clamping pressure. The top S surface perpendicular to the bonded interface was polished for the indentation tests. A linear sequence of indentations was made with a sphere of radius $r = 1.98$ mm, with the contacts centered across the interface trace, at peak loads again up to $P = 3000$ N. The two halves of the indented specimens were then separated by

Table I. Compositions and Thicknesses of Silicon Nitride Laminates of Homogeneous Si_3N_4 S and Heterogeneous Si_3N_4 :BN B Layers (Fig. 1)

Laminate	Wt% BN in B	d_s (μm)	d_b (μm)
SB10(1)	10	150	70
SB10(2)	10	60	70
SB30(1)	30	50	50
SB30(2)	30	50	20

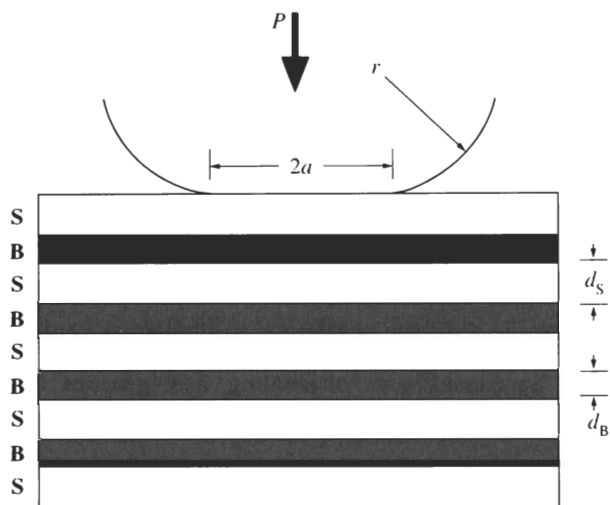


Fig. 1. Schematic of multilayer laminate with alternating Si_3N_4 (S) and silicon nitride/boron nitride composite (B) layers, thicknesses d_s and d_b . Laminate is subjected to Hertzian contact with WC sphere of radius r at load P , contact radius a .

dissolving the glue in acetone, cleaned, gold-coated, and examined using a reflection optical microscope in Nomarski interference illumination.

III. Results

(1) Laminate Characterization

X-ray diffraction analysis of the laminates confirmed the presence of hexagonal BN as a dominant second phase in the Si_3N_4 laminates. SEM microscopic examination of the sections showed the BN to exist as platelets in the B layers,^{2,10} with dimensions 2 to 5 μm diameter and 0.2 to 0.6 μm thickness. Radial cracks from the exploratory Vickers indentations in the B30 composite material deflected abruptly on intersection with these platelets (Fig. 2), indicating weak BN/ Si_3N_4 interphase boundaries. Porosities 3.1% and 4.3% were measured in the B10 and B30 materials, respectively, substantially lower than the 10% to 30% levels previously reported for Si_3N_4 composites with the same BN content.^{9,10}

The laminate microstructure is revealed most clearly in plasma-etched sections. Figure 3 shows the etched region between adjacent S and B layers for an SB10 laminate. The large elongate voids in the B30 layer are the remnants of BN

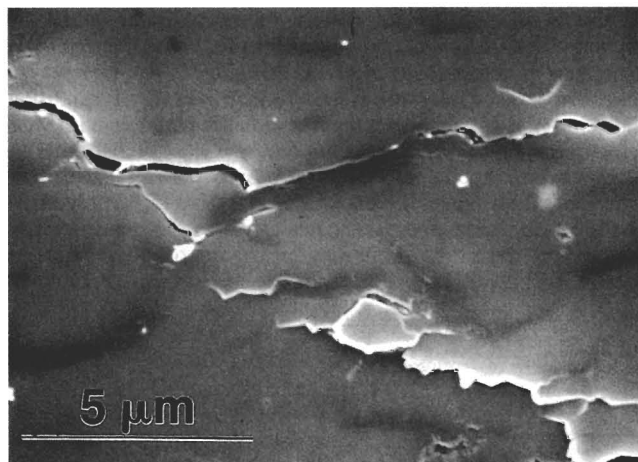


Fig. 2. Radial crack from Vickers indentation in top surface of B30 composite material. Note deflection of crack at boundaries of BN platelets (dark, elongate phase) with matrix Si_3N_4 .

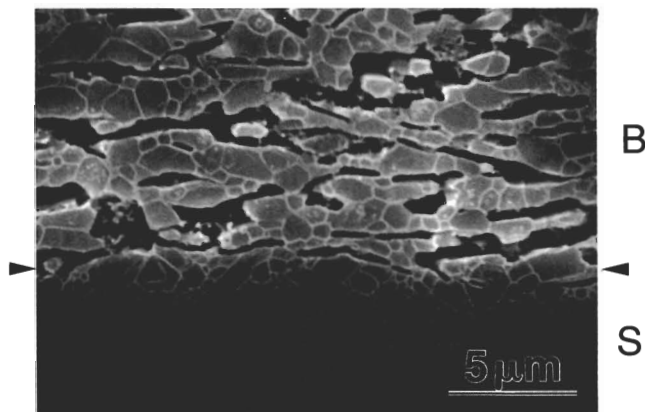


Fig. 3. SEM micrograph of plasma-etched section of interlayer interface region in SB10 multilayer. Note well-defined void-free interface (arrows) between S layer and B layer. BN platelets are indicated by remnant elongate voids in B layer, dislodged during plasma etching.

platelets. The BN platelets have a large basal-plane coefficient of thermal expansion relative to Si_3N_4 and are therefore loosely held in the matrix. There is a strong alignment of the elongate voids parallel to the S/B interface, partly from the hot pressing, so the B microstructure is textured. These elongate voids are almost contiguous in the B30 layer, accounting for the quality of “machinability” exhibited by this composite material.⁹ Most importantly, the Si_3N_4 matrix is continuous across the S/B interface, implying strong interlayer bonding.

(2) Hertzian Indentation Stress–Strain Curves

Indentation stress–strain data are plotted for SB10 and SB30 laminates in Figs. 4 and 5, respectively. The solid curves are empirical fits. In each figure, the curves for free-standing bulk Si_3N_4 S and Si_3N_4 :BN B materials constitute upper and lower bounds to the SB composite laminate response. For the S material, the response is near-linear up to ≈ 7 GPa,¹⁹ above which irreversible deformation occurs in the specimen (as well as in the tungsten carbide sphere.¹²) For the B materials, the response departs markedly from linearity at a comparatively low stress level, < 1 GPa, corresponding to a substantial depression in yield stress, the more so for B30 in Fig. 5. These results indicate that the BN confers considerable plasticity to the Si_3N_4 matrix, similar to the effect of platelet additions in other ceramics.^{8,13,14,34}

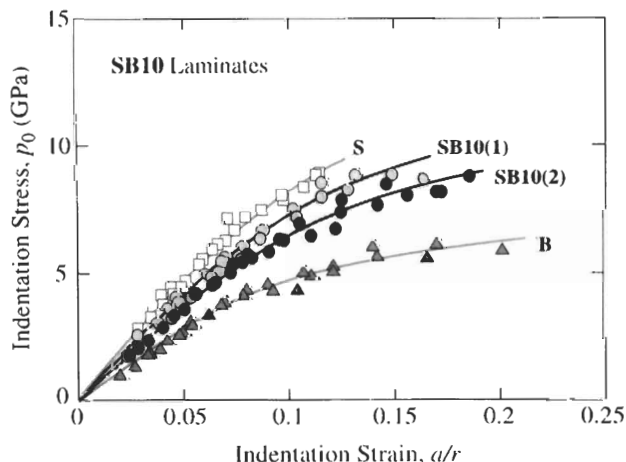


Fig. 4. Indentation stress–strain curves for SB10 bonded-interface multilayer specimens: (1) $d_s = 150 \mu\text{m}$ and $d_b = 70 \mu\text{m}$; (2) $d_s = 60 \mu\text{m}$ and $d_b = 70 \mu\text{m}$. Data included for bulk Si_3N_4 S and composite B material as limiting cases. Solid curves are empirical fits.

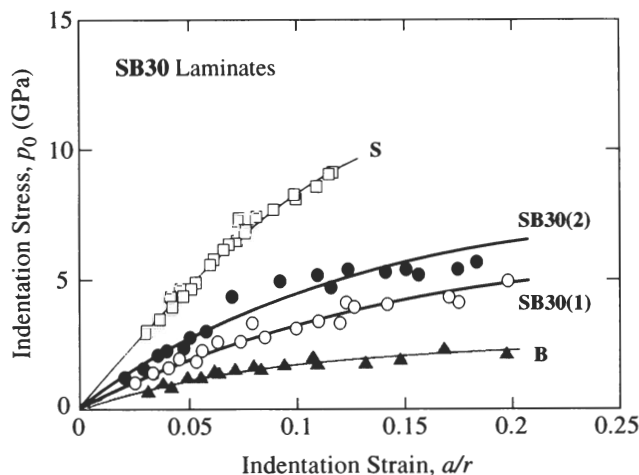


Fig. 5. Indentation stress–strain curves for SB30 bonded-interface multilayer specimens: (1) $d_b = 50 \mu\text{m}$ and $d_s = 50 \mu\text{m}$; (2) $d_s = 50 \mu\text{m}$ and $d_b = 20 \mu\text{m}$. Data included for bulk Si_3N_4 S and composite B material as limiting cases. Solid curves are empirical fits.

For the composite SB laminates in Figs. 4 and 5 the stress–strain curves lie between the S and B bounds, seemingly corresponding to some kind of rule-of-mixtures additivity. In this context it may be noted that the range of contact diameters corresponding to the data in Figs. 4 and 5 extends up to $\approx 800 \mu\text{m}$, considerably larger than the layer thicknesses (see Figs. 6 and 7, below). The shift away from the S toward the B curve is more pronounced in the SB30 than in the SB10 laminates, and at larger d_b/d_s , again pointing to an increase in plasticity with BN content. Note that, over the data range, the maximum stresses achieved in the laminates barely exceed 7 GPa in SB10, and do not even closely achieve this level in SB30, implying that the plastic strains are confined almost exclusively to the B layers.

(3) Hertzian Contact Damage

Bonded-interface specimens were used to provide section views of the subsurface Hertzian contact damage in the SB laminates. Preliminary tests on free-standing bulk materials revealed cone cracks in the tensile zone outside the contact in the bulk Si_3N_4 and, conversely, distributed quasi-plastic deformation in the shear zone beneath the contact in the bulk Si_3N_4 :BN, similar in form to the damage patterns observed in other ceramics with incorporated platelet microstructures.^{8,13,14,34} and consistent with the softening trend noted in the preceding subsection.

Figure 6 shows a section from a bonded-interface specimen of SB10 laminate, $d_s = 150 \mu\text{m}$ and $d_b = 70 \mu\text{m}$, after Hertzian contact at a peak load $P = 2000$ N (equivalent indentation strain $a/r = 0.133$ —cf. Fig. 4). Not unexpectedly, the damage takes on an altogether different form in the two kinds of material layer. A partial cone crack initiates in the outer homogeneous S layer, but does not penetrate through to the underlayer. The depth of this partial cone crack is much less than that formed in the bulk Si_3N_4 under identical contact conditions—it is as if the cone crack field becomes “shielded” from the applied loading as it approaches the softer B underlayer.³⁴ The damage in the B layer is more distributed, in the form of shear faults along the Si_3N_4 /BN matrix/platelet interfaces and ensuing microcracks,^{13,14,34} coalescing into an inverted intra-layer saucerlike failure locus that ultimately traverses the layer. The traditional interlayer delamination is not observed. At intersection with the lower interlayer interface, the stress concentration from this failure locus initiates another partial cone crack in the subsequent S layer, and so on. Hence, the softer B layer is able to transmit fracture through the structure, but not without substantial quasi-plastic energy absorption, much as across metal interlayers in ceramic/metal laminates.³⁵

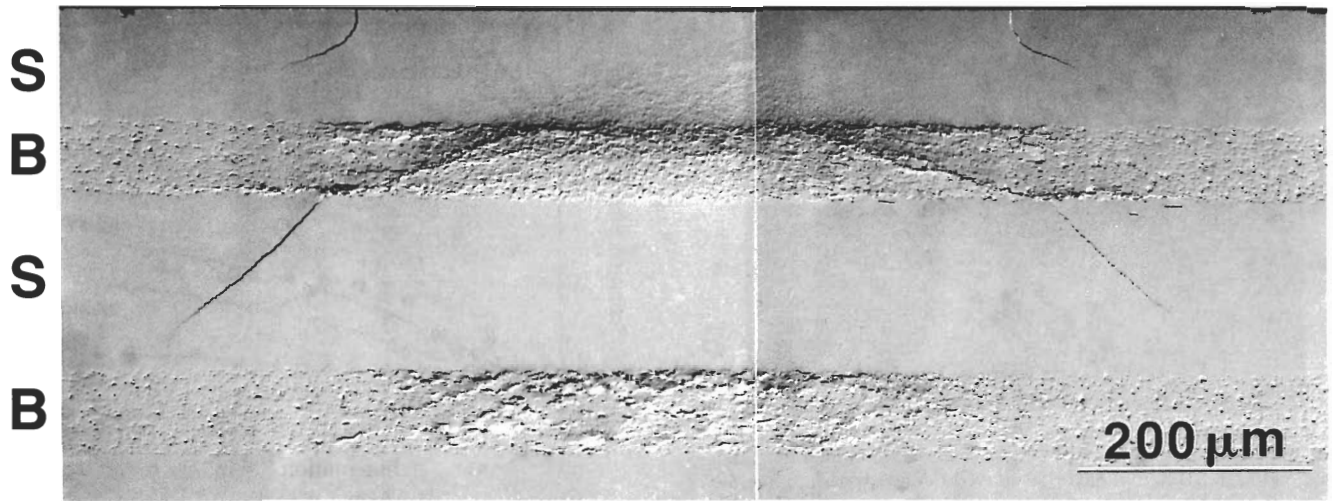


Fig. 6. Nomarski optical micrographs of subsurface damage in SB10 bonded-interface multilayer specimen. $d_s = 150 \mu\text{m}$ and $d_b = 70 \mu\text{m}$, after Hertzian contact with WC sphere radius $r = 1.98 \text{ mm}$ at load $P = 1500 \text{ N}$ ($a/r = 0.117$). Note partial cone cracks in S layers 1 and 3, and saucerlike failure in B layers 2 and 4.

Figure 7 shows a sequence of sections of an SB30 laminate, $d_s = 50 \mu\text{m} = d_b$, with expanding Hertzian contact. The damage pattern is similar to that in Fig. 6, only more severe, owing to a higher net BN content (cf. Figs. 6 and 7(c) at the same load). We note the following sequence of damage evolution with increasing load (equivalent indentation strain a/r indicated in the caption, to enable comparison with Fig. 5): (a) $P = 500 \text{ N}$, the onset of saucerlike failures in the first three B underlayers, but no cone cracks in any of the S overlayers;

(b) $P = 1000 \text{ N}$, initiation of downward-extending partial cone cracks in the first two or three S layers, the first at the top free surface and the others at the lower-outer edges of the saucerlike failures at the B/S interfaces—in addition, initiation of a second set of upward-extending stable cracks at the upper edges of the saucerlike failures; (c) $P = 1500 \text{ N}$, continued intensification of the damage to more underlayers, with increasing densities of partial cone cracks and stable intralayer cracks; (d) $P = 2000 \text{ N}$, continued increase in damage and crack severity; (e) $P =$

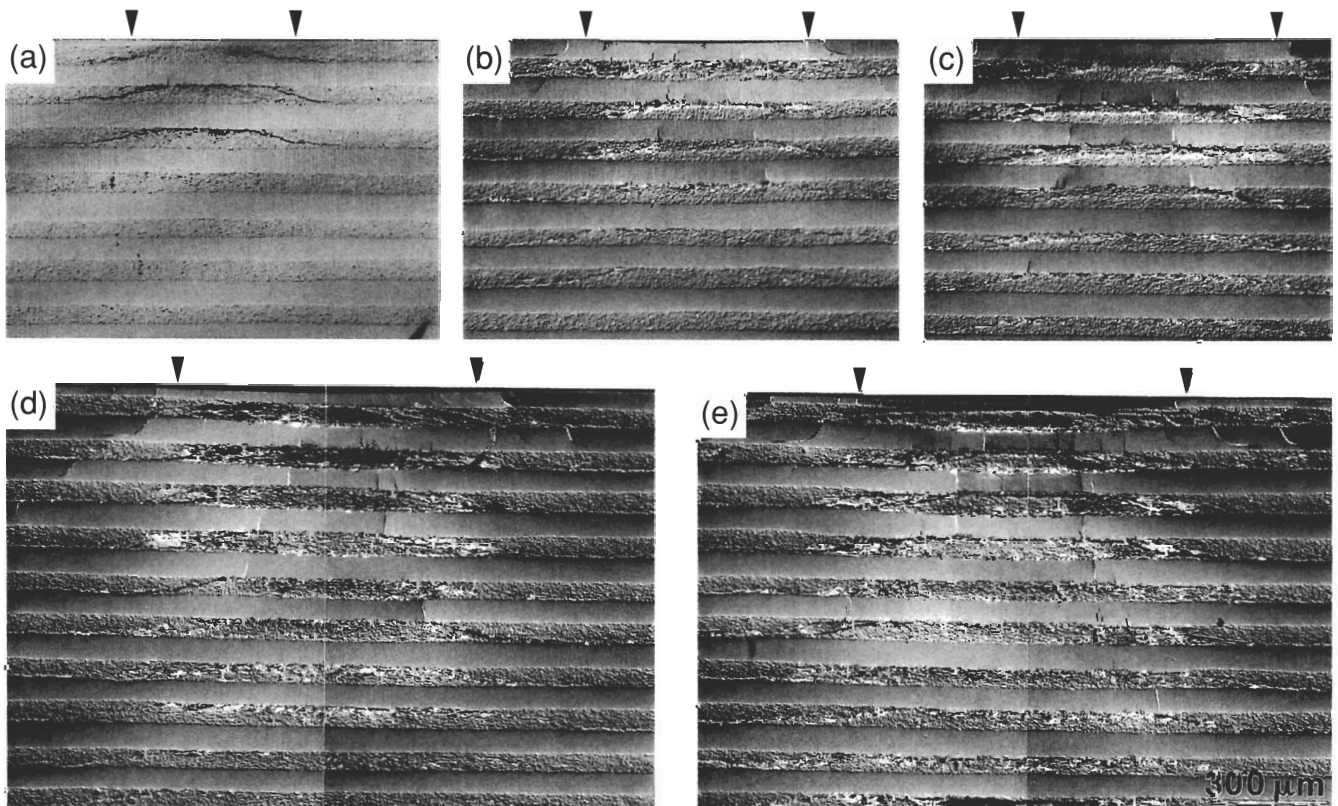


Fig. 7. Nomarski optical micrographs of subsurface damage in SB30 bonded-interface multilayer specimen. $d_s = 50 \mu\text{m}$ and $d_b = 50 \mu\text{m}$, after Hertzian contact with WC sphere radius $r = 1.98 \text{ mm}$, at loads: (a) $P = 500 \text{ N}$ ($a/r = 0.109$), (b) $P = 1000 \text{ N}$ ($a/r = 0.142$), (c) $P = 1500 \text{ N}$ ($a/r = 0.168$), (d) $P = 2000 \text{ N}$ ($a/r = 0.189$), (e) $P = 2500 \text{ N}$ ($a/r = 0.209$). Arrows indicate contact diameter. Note partial cone cracks and secondary upward-extending cracks contained within S layers, and damage accumulation and saucerlike failure in B layers. Note that at the higher loads in this sequence the damage takes on the form of a macroscopic quasi-plastic zone beneath the contact.

2500 N, an indication that some of the cracks are on the verge of traversing individual S layers. Ultimately, at some load between 2500 and 3000 N, a strong load drop was noted in the applied loading system, although even then the specimen remained intact. The capacity of the laminate system to sustain plastic strain is evident from the very apparent residual surface contact depressions in this sequence, especially at the higher loads. The depth of damage is also considerable, substantially deeper than corresponding damage in bulk homogeneous Si_3N_4 under equivalent loading conditions.¹⁹

IV. Discussion

We have demonstrated the capacity of tailored silicon nitride laminates for absorbing and distributing damage in large-scale Hertzian contacts. The key to the damage tolerance lies in the alternation of homogeneous Si_3N_4 S overlayers with heterogeneous Si_3N_4 :BN B underlayers, with strong S/B interlayer bonding. As seen in Figs. 4 and 5, the BN "softens" the Si_3N_4 matrix, rendering the B underlayers energy-absorbing and tough and thereby highly effective in crack attenuation. At the same time, the relatively hard and stiff S outer material preserves the wear resistance of the Si_3N_4 material.

Widely distributed damage is evident in the subsurface contact zones of Figs. 6 and 7. Multiple cracking occurs even in the brittle homogeneous S layers, most notably in the near-surface levels. Below $P = 2500$ N, where the first load drops begin, this cracking is highly confined, indicating some kind of shielding of the applied load by the softer B layers.³⁴ At the periphery of the damage zone, partial cones propagate downward, but do not penetrate to the lower S/B interface. Within the inner regions of the damage zone, secondary cracks propagate upward, but again remain stable within the intralayer. These cracks may be driven by tensile "plate" stresses in the upper-edge and lower-center regions of the cushioned S layers immediately below the contact area, and at the same time may be stabilized by compressive stresses from the greater Hertzian field, much as in the indentation of hard coatings on compliant substrates.³⁷

The intensive damage within the heterogeneous B layers is microscopically diffuse. As indicated, the additive BN platelets have weak interphase boundaries and large thermal expansion mismatch with the Si_3N_4 matrix, ideal microstructural ingredients for promoting "quasi-plastic" deformation in otherwise brittle ceramics.^{8,13-15,34} Individual microdeformation events can be modeled in terms of shear-driven frictional sliding at the weak interfaces, leading to interface microfailures.³⁸ Such microfailures account for the "machinability" of those ceramics in which the platelets form contiguous networks.^{2,15,39,40} However, the manner in which these individual events coalesce into the macroscopic inverted saucerlike failure loci in the B layers in Figs. 6 and 7 remains to be ascertained. One factor that must contribute to the tendency toward such a lateral failure mode is the lamella texture of the BN structure, although inevitably the dominant factor must be the stress state. Specific coalescence processes have been modeled in the compression failure of microcracked solids^{41,42} and the shear failure of adhesives.^{43,44} Here, the contact field contains large components of both compression and shear, although detailed evaluations of the complex elastic-plastic stress state in the soft B layers are not yet available. Such evaluations would appear to be called for, with due attention to unloading as well as to loading, in order to determine the operative stresses along the ultimate failure loci.

An important aspect of the laminate damage is the synergism evident in Figs. 6 and 7 between the interlayer modes. The B layer deformation appears on the one hand to enhance the initiation of adjacent S intralayer cracks, and at the same time to inhibit the propagation of these cracks. The net result is an alternating layer-by-layer stacking of saucerlike B layer failure loci coupled with partial S layer microfractures, punched deeply into the laminate structure by the penetrating indenter. Thus, damage can be transmitted through the subsurface contact zone, but in a highly stable and widely dispersed manner,

in direct contrast to the single cone fractures that characterize bulk homogeneous ceramics. Such dispersed damage qualities are hallmarks of tolerant structures, with considerably reduced susceptibility to contact-induced strength degradation.^{13,14} In our laminates, this tolerance would appear to derive primarily from intrinsic microstructural sources, namely the weak platelet/matrix interfaces, rather than from extrinsic sources, as previously argued from studies on relatively porous Si_3N_4 :BN materials.^{9,10} Again, by retaining a homogeneous outer layer, the wear properties of the Si_3N_4 are unlikely to be compromised. On the other hand, the microstructurally diffuse nature of the damage may render the structure somewhat more prone to fatigue failure by material comminution in repeat loading.^{21,45}

The present study raises issues, both material and geometrical, in laminate design. From the material standpoint, the key is the incorporation of a chemically stable "softening" phase into the sublayer material, here BN into matrix Si_3N_4 , to provide elastic-plastic interlayer mismatch. The retention of Si_3N_4 as a common base for both the homogeneous and the heterogeneous layers ensures a strong interlayer bond. What then is the optimum BN content in the heterogeneous layers? From the geometrical standpoint, what is the optimum thickness for each layer? Would it be beneficial to consider grading the laminates, e.g., by varying both the BN content and layer thicknesses through the structure? To some extent, the answers to such questions will depend on the scale and intensity of the prospective contact event, in the broader context of an integrated approach to materials processing, characterization, and properties.

Finally, it is acknowledged that questions of the kind raised in the previous paragraph cannot be fully addressed without a more quantitative analysis of the contact deformation process. As indicated, any such analysis, even for single-layer ceramic systems, lies beyond the range of currently available contact models.⁴⁶ It is necessary to incorporate provision for an elastic-plastic constitutive relation for either one or both of the laminate materials. The geometrical complexity of the ensuing contact configuration would appear to necessitate recourse to numerical analytical techniques, such as finite-element modeling.^{37,47} Initial studies of this kind for ceramic systems are under way.^{48,49}

Acknowledgments: We thank Antonia Pajares, Anthony Fischer-Cripps, and Hockin Xu for assistance with the contact experiments, and Jay Wallace with the plasma etching experiments.

References

- B. R. Lawn, *Fracture of Brittle Solids*; Ch. 7. Cambridge University Press, Cambridge, U.K., 1993.
- E. Tani, S. Umebayashi, K. Kiashi, K. Kobayashi, and M. Nishijima, "Gas-Pressure Sintering of Si_3N_4 with Concurrent Addition of Al_2O_3 and 5 wt% Rare Earth Oxide: High Fracture Toughness Si_3N_4 with Fiber-Like Structure," *Am. Ceram. Soc. Bull.*, **65** [9] 1311-15 (1986).
- C.-W. Li and J. Yamanis, "Super-Tough Silicon Nitride with R-Curve Behavior," *Ceram. Eng. Sci. Proc.*, **10** [7-8] 632-45 (1989).
- C.-W. Li, D.-J. Lee, and S.-C. Lui, "R-Curve Behavior and Strength of In-Situ Reinforced Silicon Nitride with Different Microstructures," *J. Amer. Ceram. Soc.*, **75** [7] 1777-85 (1992).
- P. L. Swanson, C. J. Fairbanks, B. R. Lawn, Y.-W. Mai, and B. J. Hockey, "Crack-Interface Grain Bridging as a Fracture Resistance Mechanism in Ceramics: I, Experimental Study on Alumina," *J. Am. Ceram. Soc.*, **70** [4] 279-89 (1987).
- Y.-W. Mai and B. R. Lawn, "Crack-Interface Grain Bridging as a Fracture Resistance Mechanism in Ceramics: II, Theoretical Fracture Mechanics Model," *J. Am. Ceram. Soc.*, **70** [4] 289-94 (1987).
- P. L. Swanson, "Crack-Interface Traction: A Fracture-Resistance Mechanism in Brittle Polycrystals"; pp. 135-55 in *Fractography of Glasses and Ceramics*, Advances in Ceramics, Vol. 22. Edited by J. Varner and V. D. Frechette. American Ceramic Society, Columbus, OH, 1988.
- B. R. Lawn, N. P. Padture, H. Cai, and F. Guiberteau, "Making Ceramics 'Ductile,'" *Science (Washington, DC)*, **263**, 1114-16 (1994).
- K. Isomura, T. Fukuda, K. Ogasahara, T. Funahashi, and R. Uchimura, "Machinable Si_3N_4 -BN Composite Ceramics with High Thermal Shock Resistance, High Erosion Resistance"; pp. 624-34 in *UNITECH '89 Proceedings*. Edited by L. J. Trostel. American Ceramic Society, Westerville, OH, 1989.
- E. H. Lutz and M. V. Swain, "Fracture Toughness and Thermal Shock Behavior of Silicon Nitride-Boron Nitride Ceramics," *J. Am. Ceram. Soc.*, **75** [1] 67-70 (1992).
- F. Guiberteau, N. P. Padture, H. Cai, and B. R. Lawn, "Indentation Fatigue: A Simple Cyclic Hertzian Test for Measuring Damage Accumulation in Polycrystalline Ceramics," *Philos. Mag. A*, **68** [5] 1003-16 (1993).